

Mosaic-skeleton approximation is all you need for Smoluchowski equations

Roman Dyachenko^{1,2}, Sergey Matveev^{2,3}, and Bulat Valiakhmetov^{2,3}

¹HSE University and Skolkovo Institute of Science and Technology, Moscow, Russia

²Marchuk Institute of Numerical Mathematics, RAS, Moscow, Russia

³Lomonosov MSU, faculty of Computational Mathematics and Cybernetics, Moscow, Russia

January 20, 2025

Abstract

In this work we demonstrate a surprising way of exploitation of the mosaic–skeleton approximations for efficient numerical solving of aggregation equations with many applied kinetic kernels. The complexity of the evaluation of the right-hand side with M nonlinear differential equations basing on the use of the mosaic-skeleton approximations is $\mathcal{O}(M \log^2 M)$ operations instead of $\mathcal{O}(M^2)$ for the straightforward computation. The class of kernels allowing to make fast and accurate computations via our approach is wider than analogous set of kinetic coefficients for effective calculations with previously developed algorithms. This class covers the aggregation problems arising in modelling of sedimentation, supersonic effects, turbulent flows, etc. We show that our approach makes it possible to study the systems with $M = 2^{20}$ nonlinear equations within a modest computing time.

1 Introduction

Aggregation is a basic natural process and plays an important role in numerous phenomena [1] including the processes at the microscale (e.g., polymerization [2,3] or dust formation [4]) and macroscale (e.g., particle formation at Saturn’s rings [5]). Series of useful facts about growing random graphs can be found in the framework of aggregation equations [6–9]. All in all, this knowledge might be useful for revealing the mechanisms of the community formation in the social networks and biological systems [10].

We study the aggregation process assuming that it is a collision-controlled process and that particles fill the space homogeneously. In such case, one may pay interest not to evolution of the distinct particles but to concentrations $n_s(t)$ of the cluster of size s per unit volume of the system. In case of pairwise collisions leading to the mass-conserving aggregation with rates $K_{ij} = K_{ji} \geq 0$ (also called kernels) the celebrated Smoluchowski equations can be derived [11,12]:

$$\frac{dn_s}{dt} = \frac{1}{2} \sum_{i+j=s} K_{ij} n_i n_j - \sum_{j=1}^{\infty} K_{sj} n_s n_j. \quad (1)$$

These balance equations correspond to the irreversible aggregation process and can be studied analytically only for very special cases of kernels and initial conditions [13]. In most applications, researchers utilize the numerical methods that allow one to approximate the solution with some finite accuracy. Today, there exist many fundamentally different approaches that allow to study the aggregation equations with the use of computers [14]. Namely, they can be finite-difference [15–17], finite-volume [18], direct simulation Monte Carlo approaches [19–23], the specific coarse graining tricks [24,25] and even the homotopy perturbation methods [26]. Each of these methods has its specific advantages and drawbacks. For example, the direct simulation Monte Carlo methods naturally fulfill the mass

conservation laws, but their accuracy is limited. On the other hand, the deterministic finite-difference approach is very accurate but might be resource-consuming. Coupling of the finite-difference methods with the ideology of the low-rank decomposition allows to partially solve this problem and perform extremely accurate simulation within modest times [15–17]. However, there are still classes of aggregation kernels that do not have exactly or numerically low rank. Some examples of these kernels are the following:

$$K_{ij} = \begin{cases} (i^{1/3} + j^{1/3})^2 |i^{2/3} - j^{2/3}|, & i \neq j, \\ (i^{1/3} + j^{1/3})(i^{-1/3} + j^{-1/3}), & i = j. \end{cases} \quad (2)$$

$$K_{ij} = \begin{cases} \frac{(i+j)(i^{1/3} + j^{1/3})^{2/3}}{(ij)^{5/9} |i^{2/3} - j^{2/3}|}, & i \neq j, \\ (i^{1/3} + j^{1/3})(i^{-1/3} + j^{-1/3}), & i = j. \end{cases} \quad (3)$$

Such kernels (see e.g. (2)) may arise in problems with spatially inhomogeneous aggregation of particles moving within some stream. Surprisingly, the popular and fine-tuned Monte Carlo approaches also degenerate in terms of efficiency for the problems with such kernels. It motivates us to revisit and reformulate the methodology utilizing low-rank matrix structures for the more general class of matrices with low mosaic rank.

In our work, we extend the previously proposed approach [27] through the application of the adaptive cross methods [28–31] for the mosaic approximation of the kinetic coefficients. This idea allows us to solve huge systems of up to 2^{20} equations with no need for supercomputing facilities. We also confirm the efficiency of our approximations for a large number of kernels encountered in practice and conduct the convergence analysis in comparison with the family of Monte Carlo methods.

The main contributions of our work are:

- great compression rate on a broad family of coagulation kernels within the mosaic–skeleton format;
- new algorithms for efficient evaluation of the Smoluchowski operator based on the mosaic-skeleton structure;
- incorporation of the adaptive cross approximation allowing to deal with huge systems of aggregation equations;
- an open high-performance solver for solving Smoluchowski equations ¹.

2 Approximation of kernels

Let us describe the scheme for modeling the coagulation process using (1). We first consider a coagulation equation with the particle size limit set as M :

$$\frac{dn_s}{dt} = \frac{1}{2} \underbrace{\sum_{i+j=s} K_{ij} n_i n_j}_{f_1(s)} - \underbrace{\sum_{j=1}^M K_{sj} n_s n_j}_{f_2(s)}, \quad s = 1, \dots, M. \quad (4)$$

Such system of ODEs can be solved with various time-integration approaches. Nevertheless, in order to perform the time-step one has to calculate the operators $f_1(s)$, $f_2(s)$ for all $s = 1, 2, \dots, M$.

It is easy to see that the direct calculation requires $\mathcal{O}(M^2)$ arithmetic operations for both f_1 and f_2 terms. However, in recent years, some efficient methods have been developed [15, 16, 32]. These approaches utilize low-rank approximations of the kernel to speed up the calculation of f_1 and f_2 .

¹<https://github.com/DrEternity/FDMSk-Smoluchowski>

2.1 Low-rank method

In this section we show a certain approach allowing to speedup computation of the operators f_1 and f_2 from Eq. (4). At first, we construct a low-rank decomposition of the coagulation kernel:

$$K_{ij} \approx \sum_{\alpha=1}^R U_{i\alpha} V_{j\alpha}, \quad (5)$$

$$K \approx UV^\top, \quad (6)$$

where $U, V \in \mathbb{R}^{M \times R}$. Any relevant approach can be used for construction of U and V e.g. the singular value decomposition (SVD) [33], its randomized version [34] or the adaptive cross approximation [28–31].

The adaptive cross method allows one to deal with function-generated matrices and has a linear complexity $\mathcal{O}(MR^2)$ with respect to the matrix size M . These two features allow us to approximate kernels for systems with up to $M = 2^{20}$ equations.

As soon as the low-rank decomposition is constructed, we obtain the relation for the first operator:

$$f_1(s) = \frac{1}{2} \sum_{i+j=s} K_{ij} n_i n_j = \frac{1}{2} \sum_{i+j=s} \sum_{\alpha=1}^R U_{i\alpha} V_{j\alpha} n_i n_j = \frac{1}{2} \sum_{\alpha=1}^R \sum_{i+j=s} [U_{i\alpha} n_i] [V_{j\alpha} n_j].$$

It is the sum of R vector convolutions:

$$f(s) = \sum_{i+j=s} g(i)h(j).$$

Each summand can be calculated within $\mathcal{O}(M \log M)$ operations using the fast Fourier transform.

For the second operator, we obtain the following relation:

$$f_2(s) = n_s \sum_{j=1}^M K_{sj} n_j = n_s \sum_{j=1}^M \sum_{\alpha=1}^R U_{s\alpha} V_{j\alpha} n_j = n_s \sum_{\alpha=1}^R U_{s\alpha} \sum_{j=1}^M V_{j\alpha} n_j.$$

Or in matrix form it can be written like this:

$$f_2 = n \odot (UV^\top n),$$

where U and V are the factors of the skeleton decomposition, n is an input vector and \odot is an element-wise product. Evaluation of the whole vector f_2 requires $\mathcal{O}(MR)$ operations.

Thus, we obtain a numerical approach for calculation of the Smoluchowski operator within $\mathcal{O}(RM \log M)$ operations instead of the initial $\mathcal{O}(M^2)$.

Final structure of the numerical method exploiting the low-rank representations of the aggregation coefficients requires some time-integration scheme. In this work, we utilize the classical Runge–Kutta–Fehlberg method [35,36].

The quality of the low-rank approximations of matrix K in the Frobenius norm corresponds to the decrease of its singular values. Let $A = U\Sigma V^\top \in \mathbb{R}^{m \times n}$, $m \leq n$, be the singular value decomposition of A , where $\Sigma = \text{diag}(\sigma_1, \dots, \sigma_m)$ and U, V^\top – orthogonal matrices. Taking the truncated matrices U_r, V_r as the first r columns of U and V and truncating $\Sigma_r = \text{diag}(\sigma_1, \dots, \sigma_r)$, we obtain the rank- r matrix $A_r = U_r \Sigma_r V_r^\top$. A_r is an optimal approximation of A in terms of the Frobenius norm:

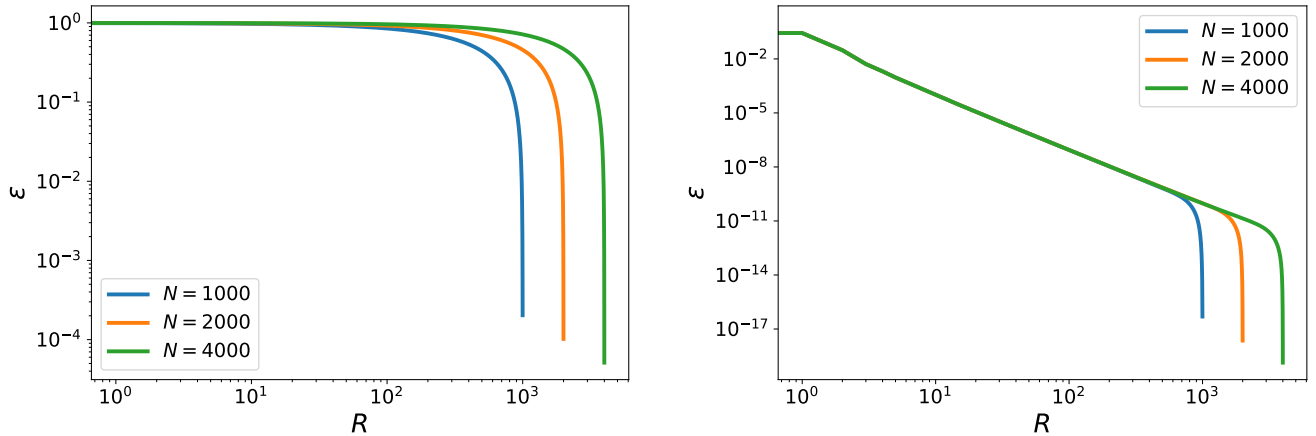
$$\|A - A_r\|_F = \min_{\text{rank}(B) \leq r} \|A - B\|_F = \sqrt{\sigma_{r+1}^2 + \dots + \sigma_m^2}.$$

This expression for the value of the approximation error is known as the famous Eckart–Young–Mirsky theorem (see e.g. [33]).

Hence, if the “tail” $\sigma_{r+1}, \dots, \sigma_m$ of the singular values decreases rapidly, then the whole matrix can be accurately approximated with a low-rank one. The family of such matrices is rather broad and includes a lot of function-generated matrices [37] and also positive semidefinite Hankel matrices [38].

An approach basing on low-rank matrix approximations can be applied successfully to a wide class of applied phenomena related to aggregation kinetics. The list of possible kernels includes the ballistic [39–41], Brownian [42–44], and others [3, 5, 45]. However, many kernels (for example given by Eqs. (2) and (3)) [46–51] cannot be approximated via the low-rank format.

The slow decrease of the singular values of the kernels (2) and (3) can be seen on Figure 1. This trouble inspires us to extend the existing approach using the wider class of low parametric matrices for solving the Smoluchowski-class equations.



$$(a) K_{ij} = \frac{(i+j)(i^{1/3} + j^{1/3})^{2/3}}{(ij)^{5/9} |i^{2/3} - j^{2/3}|}$$

$$(b) K_{ij} = (i^{1/3} + j^{1/3})^2 |i^{2/3} - j^{2/3}|$$

Figure 1: Smoluchowski kernels low-rank approximation error in the Frobenius norm depending on the rank R for different matrix sizes N

2.2 Mosaic-skeleton approximations

Mosaic-skeleton matrix representation emerged as a way allowing to approximate function generated matrices, in particular the matrices related to the integral operators [52, 53]. This format is also known as a hierarchical format [54] or \mathcal{H} -matrix representation.

In general, the matrix K can be considered as the table of some function values:

$$K_{ij} = f(y_i, x_j).$$

If $f(y, x)$ is smooth enough and two sets of values $Y = \{y_i\}$, $X = \{x_j\}$ correspond to some quasi-uniform spatial grids, then K may be well approximated within the low-rank format (6). In particular, it is known that for the *asymptotically smooth* functions the corresponding matrices can also be described with modest number of parameters growing almost linearly with respect to its size [55]. Hence, the mosaic-skeleton format may be considered as an extension of basic low-rank representation.

Let us consider the whole matrix describing the full set of pairwise interactions between entries of sets Y and X defined by the elements of K . For the sake of finding the low-rank structure, we can split each of them into two smaller subsets and check its presence at four new blocks. If some of them cannot be approximated, then we split those ones recursively. One has to continue this splitting procedure until each new block can be approximated precisely via basic skeleton format or its size is small enough. These small blocks have to be evaluated and stored fully, as dense matrices. Finally, the matrix K is split into blocks of different sizes and formats (either dense or the low-rank (6)). We name such blockwise structure the mosaic-skeleton format and present it schematically in Figure 2.

There are some key questions to clarify such procedure:

1. How to split blocks (and corresponding spatial points of sets Y and X)?
2. How to determine whether the block has numerically low rank or not?
3. How to get the approximation factors U and V for every block of such kind?

Complete implementation details and nuances of the general algorithm could be found in different papers [54, 56, 57]. In our case, we utilize the basic version of the algorithm constructing the mosaic-skeleton approximation.

Since the aggregation kernel elements K depend on indices in a straight-forward way, the points of Y and X are set as $x_i \equiv y_i \equiv i \in \{1, 2, \dots, M\}$. The questions listed above get the following answers:

1. For each block its splitting (if necessary) is provided just by halves of rows and columns. It produces four quarter blocks.
2. We choose the following criteria allowing to determine the low-rank blocks: (a) only diagonal blocks are marked as dense; (b) only diagonal, sub-diagonal and super-diagonal blocks are dense. All blocks except these are treated as low-rank. These two options lead to different mosaic partitionings depicted on Figure 2.
3. We construct the approximation of blocks that are expected to have numerically low rank using the adaptive cross approximation procedure described in the paper [30]. This algorithm allows to avoid the storage of full submatrices in memory, and evaluates the approximation “on-the-fly”.

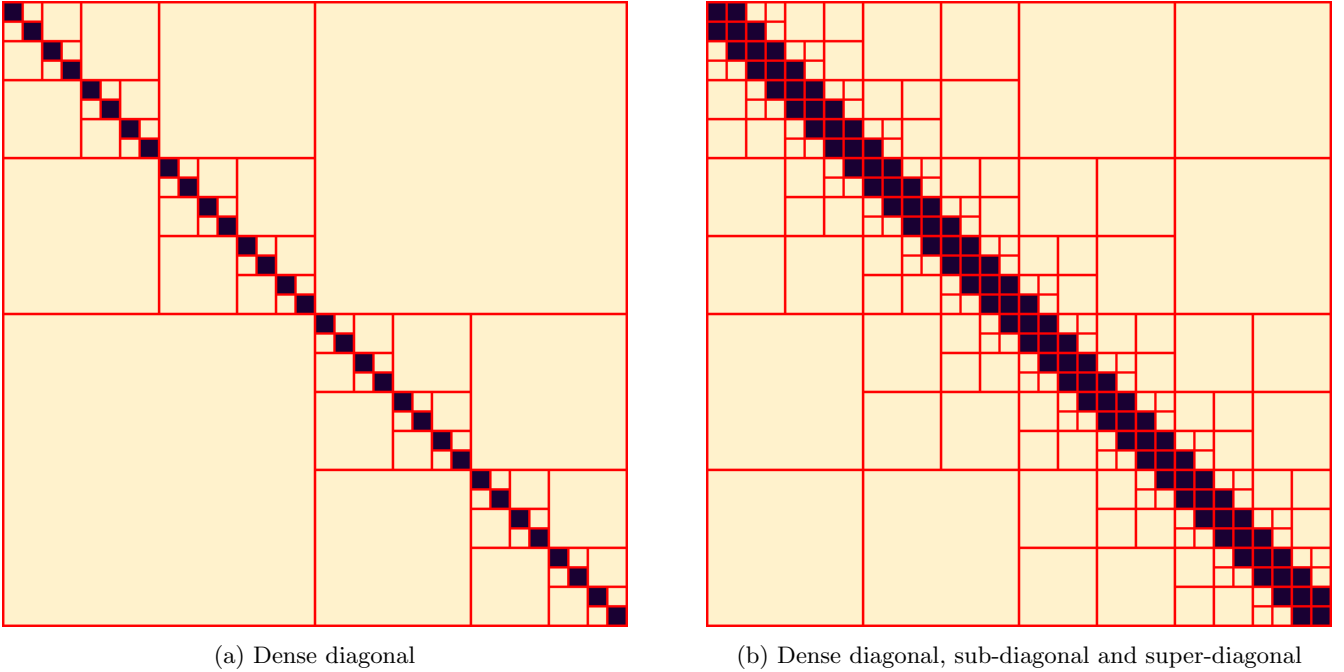


Figure 2: Mosaic partitioning depending on the low-rank criteria

In Table 1 we present some examples of kernels from different studies with their compression rate and maximal rank of a block in the mosaic-skeleton format. In these experiments we consider both mosaic partitioning options. Approximation is obtained with relative accuracy $\varepsilon = 10^{-6}$ and 10^{-12} in the Frobenius norm. The final compression rate is measured with respect to dense matrix with M^2 entries.

The described approach for approximation of the aggregation kernels demonstrates an excellent result. In the worst case, the rank 8 is enough to achieve a relative accuracy of 10^{-12} , for each complex kernel from Table 1.

These results show the versatility of our methodology and allow to apply our approach as a black-box solution for numerical modelling with a wide class of the aggregation kernels.

$K_{ij} \backslash \varepsilon$	Partitioning 1		Partitioning 2		Source
	10^{-6}	10^{-12}	10^{-6}	10^{-12}	
$(i^{1/3} + j^{1/3})^2 i^{2/3} - j^{2/3} $	5(0.01)	5(0.01)	4(0.03)	5(0.06)	aggregation within flow [4, 58–60]
$\frac{(i+j)(i^{1/3} + j^{1/3})^{2/3}}{(ij)^{5/9} i^{2/3} - j^{2/3} }$	15(0.04)	34(0.07)	4(0.04)	8(0.06)	baseline example
$(i^{1/3} + j^{1/3})^2 i^{2/3} - j^{2/3} \operatorname{erf}\left(\frac{ i^{2/3} - j^{2/3} }{\sqrt{i^{1/3} + j^{1/3}}}\right)$	7(0.02)	14(0.02)	4(0.03)	8(0.05)	modified flux reaction rates [50]
$(i^{1/3} + j^{1/3})^{5/2} \exp\left[-\frac{(i^{2/3} - j^{2/3})^2}{i^{1/3} + j^{1/3}}\right]$	7(0.02)	13(0.02)	5(0.03)	8(0.05)	modified flux reaction rates [50]
$(i^{2/3} + j^{2/3})\sqrt{(i^{2/9} + j^{2/9})} \exp\left[-c\left(\frac{i^{1/3}j^{1/3}}{i^{1/3} + j^{1/3}}\right)^4\right]$	5(0.01)	10(0.01)	4(0.03)	8(0.05)	emulsion coalescence [27, 61]
$(i^{1/3} + j^{1/3})^2 \sqrt{\frac{1}{i} + \frac{1}{j}}$	4(0.01)	7(0.01)	3(0.03)	6(0.04)	ballistic kernel [13]
$K_{ij} = (i^{1/3} + j^{1/3})^2 \cdot \left \frac{1}{i} - \frac{1}{j}\right $	3(0.01)	6(0.01)	3(0.03)	5(0.04)	modified ballistic kernel [60]
$(i^{1/3} + j^{1/3})^2 \cdot \left \frac{1}{1 - \mathbf{i} \cdot i^{2/3}} - \frac{1}{1 - \mathbf{i} \cdot j^{2/3}}\right $	4(0.01)	4(0.01)	3(0.03)	4(0.04)	orthokinetic interaction [47, 62, 63]
$\frac{i^{2/3}j^{2/3}}{i^{1/3} + j^{1/3}}$	3(0.01)	6(0.01)	3(0.03)	5(0.04)	hydrodynamic interaction [47, 63]
$(i^{1/3} + j^{1/3})^2 \sqrt{i^{1/3} j^{1/3}} \exp\left[-c(i^{1/3}j^{1/3})^{1/3}\right]$	4(0.01)	6(0.01)	3(0.03)	6(0.04)	coalescence of fluid particles (bubbles and drops) [46, 64]
$(i^{1/3} + j^{1/3})^2 \sqrt{(i^{2/3} + j^{2/3})}$	3(0.01)	6(0.01)	3(0.03)	6(0.04)	coalescence of fluid particles (bubbles and drops) [65]

Table 1: Maximal rank of a block (compression rate %) of different kernels in the mosaic–skeleton format. The constant c can have different values in different kernels. For more details, see the source in the list of references.

3 Mosaic–skeleton acceleration of Smoluchowski operator computation

A common way to solve a system of ODE numerically is to integrate it with some finite difference scheme. In particular, a family of Runge–Kutta methods allows to utilize the adaptive time-steps [36]. In our case, the most time consuming operation is the evaluation of the right–hand side of the equation. Hence, this Section is devoted to its reduction.

The Smoluchowski operator consists of two parts: $f_1(s)$ and $f_2(s)$ for $s = 1, \dots, M$, defined in Eq. (4). In Section 2.1 we show how the low–rank structure of a kernel can be used for their fast evaluation. Such trick

reduces the complexity of evaluation of $f_1(s)$ and $f_2(s)$ from quadratic to sublinear. Further, we demonstrate how to accelerate similar computations but for kernels allowing low-parametric representation in mosaic–skeleton format, described in the previous Section 2.2. Utilization of this structure allows to get almost the same asymptotic acceleration but for the broader family of kernels.

For convenience, we use the notations in agreement with the original paper [55]. Let the mosaic matrix K be composed of blocks B_p , $p = 1, \dots, P$. Denote $\Gamma(B_p)$ the matrix that coincides with K on the block B_p and has zeroes elsewhere. Then we get the following representation for the kernel:

$$K = \sum_{p=1}^P \Gamma(B_p). \quad (7)$$

Next, for the mosaic–skeleton matrix K we define its mosaic rank:

$$\text{mrank } K = \frac{1}{2M} \text{mem } K = \frac{1}{2M} \sum_{p=1}^P \text{mem } B_p, \quad (8)$$

where $\text{mem } B_p$ is the number of memory cells required for storing the representation of the block B_p . Here we assume that all blocks are square. Thus, for the block of size $m_p \times m_p$ and rank $B_p = r_p$ its number of parameters equals $\text{mem } B_p = \min(m_p^2, 2r_p m_p)$. This concept extends the classical definition of the matrix rank in terms of the number of parameters stored and also matrix-by-vector multiplication complexity, see Section 3.1.

As soon as definition is given, we need to find a relation between the mosaic rank and the matrix size M . The common approach is to assume that the rank of every block (except dense ones) is bounded by some constant:

$$\text{rank } B_p \leq R.$$

For our mosaic partitioning types (see Figure 2) the total number of blocks of size $\frac{M}{2^k} \times \frac{M}{2^k}$ is proportional to 2^k for every $k = 1, \dots, L$. Here $L = \log_2 M - k_0$ is the number of rows and columns bisection levels. Then the low–rank blocks require not more than

$$\sum_{k=1}^L 2^k \cdot R \frac{M}{2^k} = \mathcal{O}(RM \log M)$$

memory cells, where R is the maximal rank among all blocks. The number of dense blocks of size $\frac{M}{2^L} \times \frac{M}{2^L}$ is also proportional to 2^L (they can be of the smallest size only), which requires the following number of parameters for them:

$$\mathcal{O}\left(2^L \cdot \left(\frac{M}{2^L}\right)^2\right) = \mathcal{O}(2^{k_0} M) = \mathcal{O}(M).$$

Thus, the total number of parameters for the mosaic–skeleton representation of the kernel ($\text{mem } K$) is bounded by $\mathcal{O}(RM \log M)$, and from (8) it follows that the mosaic rank of K is small:

$$\text{mrank } K = \mathcal{O}(R \log M). \quad (9)$$

For a vector v we also denote its slice of size l , starting from the index α :

$$v(\alpha : \alpha + l) \equiv [v_\alpha, v_{\alpha+1}, \dots, v_{\alpha+l-1}]^\top.$$

Further, matrix and vector indexing starts from one.

3.1 Second operator, matrix–vector multiplication

At first, we discuss the second component of the Smoluchowski operator because its computation is quite simple:

$$f_2(s) = n_s \sum_{j=1}^M K_{sj} n_j.$$

In the matrix–vector form, we need to evaluate:

$$f_2 = n \odot (Kn),$$

where \odot denotes element-wise product.

Using representation (7), we get the following relation:

$$f_2 = n \odot \left(\sum_{p=1}^P \Gamma(B_p) \right) n = n \odot \left(\sum_{p=1}^P \Gamma(B_p) n \right).$$

In fact, calculating every summand $\Gamma(B_p)n$, $p = 1, \dots, P$, results in the following local matrix-vector product and addition:

$$f_2(\alpha_p : \alpha_p + m_p) \leftarrow f_2(\alpha_p : \alpha_p + m_p) + B_p n(\beta_p : \beta_p + m_p).$$

Or in index form:

$$f_2(\alpha_p + s - 1) \leftarrow f_2(\alpha_p + s - 1) + \sum_{i=1}^{m_p} B_p(s, i) n(\beta_p + i - 1), \quad s = 1, \dots, m_p.$$

Here (α_p, β_p) is the upper left corner of a block B_p of size $m_p \times m_p$. Then getting

$$f_2 \leftarrow f_2 \odot n$$

finalizes the evaluation of the operator f_2 .

For a dense block, its direct multiplication by a vector costs m_p^2 operations. And for the low–rank one, it costs $2r_p m_p$ operations if FMA (Fast Multiply plus Add) is used, as was discussed in Section 2.1. So, for both of the types of block B_p this procedure requires exactly $\text{mem } B_p$ operations. Summation over all P blocks leads to the total complexity equal to $\text{mem } K$. Combining (8) and (9), we obtain:

$$\mathcal{C}_{f_2}(M) = \mathcal{O}(RM \log M), \tag{10}$$

where $\mathcal{C}_{f_2}(M)$ is the number of arithmetic operations required for computation of the operator f_2 over a vector of size M using the mosaic–skeleton format. Recall that for a low–rank kernel we had $\mathcal{O}(RM)$. The new complexity is only on a logarithmic factor higher, while it allows to consider a broader class of kernels.

3.2 First operator, convolution

The first term in Eq. (4) is defined as follows:

$$f_1(s) = \sum_{i+j=s} K_{ij} n_i n_j, \quad s = 2, \dots, M.$$

Let us denote $z = \text{conv}(y, A, x)$ the full convolution of two vectors with a kernel:

$$z_{s-1} = \sum_{i+j=s} y_i K_{ij} x_j, \quad s = 2, \dots, 2M. \tag{11}$$

Here the resulting vector z has the size $2M - 1$. For obtaining f_1 we need to evaluate its first $M - 1$ components: $f_1 = \text{conv}(n, K, n)(1 : M)$.

For the kernel K in the mosaic-skeleton format (7), convolution transforms into the following relation:

$$f_1(s) = \sum_{p=1}^P \sum_{i+j=s} \Gamma(B_p)_{ij} n_i n_j.$$

As far as $\Gamma(B_p)$ has zeroes elsewhere except for positions $(\alpha_p : \alpha_p + m_p) \times (\beta_p : \beta_p + m_p)$ of the block B_p , each of P summands can be calculated using the following formula:

$$f_1(\gamma_p : \gamma_p + l_p) \leftarrow f_1(\gamma_p : \gamma_p + l_p) + \text{conv}(n(\alpha_p : \alpha_p + m_p), B_p, n(\beta_p : \beta_p + m_p)),$$

where $\gamma_p = \alpha_p + \beta_p$ and $l_p = 2m_p - 1$. If $\gamma_p + l_p > M + 1$ then the addition is performed till the index M , or omitted at all for $\gamma_p > M$.

Convolutions with the dense block B_p is performed as it is defined in Eq. (11) requiring $2m_p^2 = 2 \text{mem } B_p$ operations. For the low-rank blocks we utilize the FFT-based procedure in the same way as it is described in Section 2.1 above. It requires $\mathcal{O}(r_p m_p \log m_p) = \mathcal{O}(\text{mem } B_p \log m_p) = \mathcal{O}(\text{mem } B_p \log M)$ operations if $\text{rank } B_p = r_p$. Summation over all P dense and low-rank blocks leads us to $\mathcal{O}(\text{mem } K \log M)$ complexity bound. Using Eqs. (8) and (9), we obtain the total complexity of operator f_1 evaluation with a kernel in the mosaic-skeleton format:

$$\mathcal{C}_{f_1}(M) = \mathcal{O}(RM \log^2 M), \tag{12}$$

the number of arithmetic operations for vector of size M . Recall that in the case of a low-rank kernel we had $\mathcal{O}(RM \log M)$, which is also now being increased by the same logarithmic factor as f_1 .

Thus, combining Eqs. (10) and (12) we obtain the total complexity for the Smoluchowski operator:

$$\mathcal{C}_{f_1+f_2}(M) = \mathcal{O}(RM \log^2 M), \tag{13}$$

for a kernel K in the mosaic-skeleton format with off-diagonal blocks rank bounded by R . There is a wide range of full rank kernels (see Table 1) used in practice, for which we can gain significant speedup while solving the Smoluchowski equations.

4 Numerical experiments

In this section we present the results of several numerical experiments allowing to investigate the properties of our algorithm. Its convergence rate and computational complexity are studied. The experiments have been carried out for various scenarios with two types of the initial particle size distributions: the monodisperse and distributions with a wide spectrum of sizes.

Further, we denote **FDMSk** our finite difference scheme with the mosaic-skeleton approximation of a kernel. The label **LRMC** corresponds to the efficient majorant Monte Carlo method [66] that we use for comparison. The alternative method also utilizes the low-rank representations of the kernel coefficients in terms of the the special majorant functions. It shows a good performance relying on the rank R of majorant function: $\mathcal{O}(R \log M)$ per collision. For more details and implementation techniques we refer to the original paper [66].

In our experiments, we consider three kernels (constant, (2) and (3)):

$$K_{ij}^1 = 2, \quad K_{ij}^2 = (i^{1/3} + j^{1/3})^2 |i^{2/3} - j^{2/3}|, \quad K_{ij}^3 = \frac{(i+j)(i^{1/3} + j^{1/3})^{2/3}}{(ij)^{5/9} |i^{2/3} - j^{2/3}|}.$$

We obtain the low-rank majorant functions for all these kernels. The first one has rank $R = 1$ itself, the second

has rank $R = 2$ and the third one can be estimated by rank $R = 6$ function:

$$K_{ij}^2 \leq \hat{K}_{ij}^2 = 2(i^{4/3} + j^{4/3}), \quad R = 2,$$

$$K_{ij}^3 = \frac{(i^{4/3} + i^{2/3}j^{2/3} + j^{4/3})(i^{1/3} + j^{1/3})^{2/3}}{(ij)^{5/9}|i-j|} \leq \hat{K}_{ij}^3 = \frac{(i^{4/3} + i^{2/3}j^{2/3} + j^{4/3})(i^{2/9} + j^{2/9})}{(ij)^{5/9}}, \quad R = 6.$$

In all experiments, we approximate blocks of the kernel K_{ij} using the mosaic partitioning from the Figure 2b and matrix cross method [30] with the relative accuracy 10^{-6} . The values of the maximal ranks of blocks are given in the Table 1. In our benchmarks, we add the time of construction of the approximation for the kernel to the total running time of the algorithm.

We perform our numerical experiments on a single node of the cluster of INM RAS [67]. All calculations for the FDMSk were performed on a single thread. The running time of the LRMC algorithm in the Table 3 recalculated, as if all calculations were performed on the single thread, due to the fact that we used averaging of several solutions to increase accuracy. The implementation of the FDMSk algorithm can be found by the link ¹.

4.1 Basic benchmark

Unfortunately, there are only a few known solutions in the analytical form for the Smoluchowski equations. For example, for the monodisperse initial conditions $n_k(t=0) = \delta_{k,1}$ with the kernel $K_{ij}^1 = 2$ such solution has been found by Smoluchowski [11]:

$$n_k(t) = \frac{1}{(1+t)^2} e^{-(k-1)\ln(1+1/t)}. \quad (14)$$

We verify that our algorithm allows to obtain an accurate numerical solution of this problem at the time point $t = 100$. We present these results in Table 2 demonstrating the dependency of the solution error on the number of equations and the time step size. The numerical error is measured in terms of the first moment M_1 , defined the following way:

$$\|n^{\text{FDMSk}} - n^{\text{Theory}}\|_{M_1} = \sum_i i \cdot |n_i^{\text{FDMSk}} - n_i^{\text{Theory}}|. \quad (15)$$

The accuracy increases with both of the parameters refinement. One may note that for some cases the error stagnates. That is because it has two components, corresponding to the mass leaking and finite difference scheme error. They are controlled by the maximal particle size and the time step, respectively. Each of them gives its own limitations, so we need to refine them simultaneously.

However, the advantages of our method cannot be fully demonstrated in such simple an example: a lot of methods show great performance basing on this classical benchmark but lose their efficiency in cases with more complicated kinetic coefficients. Below, we consider more complex kernels without known analytical solutions.

$M \backslash \Delta t$	0.5	0.1	0.05	0.01
256	$3 \cdot 10^{-2}$	$3 \cdot 10^{-2}$	$3 \cdot 10^{-2}$	$3 \cdot 10^{-2}$
512	$2 \cdot 10^{-3}$	$2 \cdot 10^{-3}$	$2 \cdot 10^{-3}$	$2 \cdot 10^{-3}$
1024	$2 \cdot 10^{-5}$	$6 \cdot 10^{-6}$	$6 \cdot 10^{-6}$	$6 \cdot 10^{-6}$
4096	$1 \cdot 10^{-5}$	$2 \cdot 10^{-7}$	$2 \cdot 10^{-7}$	$2 \cdot 10^{-7}$
16384	$9 \cdot 10^{-6}$	$1 \cdot 10^{-8}$	$9 \cdot 10^{-9}$	$9 \cdot 10^{-9}$
65536	$9 \cdot 10^{-6}$	$2 \cdot 10^{-9}$	$1 \cdot 10^{-9}$	$9 \cdot 10^{-10}$

Table 2: Relative error of FDMSk method in norm $\|\cdot\|_{M_1}$ for case (14) and $t = 100$ with M equations and time step Δt .

¹<https://github.com/DrEternity/FDMSk-Smoluchowski>

4.2 Verification with Monte Carlo

In this subsection, kernels K_{ij}^2, K_{ij}^3 are studied. We have already noted that they have a more complex structure in comparison with the constant kernel. Since there is no available analytical solution for both of these kernels, we investigate the convergence of our algorithm numerically fixing $t = 100$ for K_{ij}^3 and $t = 0.5$ in case of K_{ij}^2 . In order to do this, we check the mutual convergence of the methods of different nature: **FDMSk** and **LRMC**. The value ε_1 denotes the mutual error, measured in terms of the first moment (see Eq. (15)):

$$\varepsilon_1 = \frac{\|n^{\text{FDMSk}} - n^{\text{LRMC}}\|_{M_1}}{\|n^{\text{Ref}}\|_{M_1}} = \frac{\sum_i i \cdot |n_i^{\text{FDMSk}} - n_i^{\text{LRMC}}|}{1}.$$

Here, the first moment of solution is considered unitary since there is no leak of mass. To evaluate convergence for a particular method, we also use the second moment integral characteristic:

$$\|n\|_{M_2} = \sum_i i^2 n_i.$$

Thus, the convergence is captured by the second moment of the reference solution:

$$\varepsilon_2 = \frac{|\|n^{\text{Numerical}}\|_{M_2} - \|n^{\text{Ref}}\|_{M_2}|}{\|n^{\text{Ref}}\|_{M_2}}.$$

The accuracy of the numerical solution obtained by the different methods depends on different parameters. For **FDMSk** the accuracy depends on the number of equations M and the step of the difference scheme Δt . And for the **LRMC** it depends on the number of particles V supported in the system and the number of simulations L used for averaging [23]. In order to obtain the reference solutions we take $M = 2^{12}$, and $\Delta t^2 = 10^{-5}$, $\Delta t^3 = 10^{-2}$ for K_{ij}^2 , K_{ij}^3 respectively in case of **FDMSk**. For the **LRMC** we setup reference parameters $V = 10^7$ and $L = 10^6$.

In this numerical experiment, we again consider a monodisperse initial condition $n_k(t = 0) = \delta_{k,1}$. For both **FDMSk** and **LRMC** we setup such simulation parameters that allow to achieve the required convergence rates ε_2 and measure the mutual error ε_1 of the obtained solutions. From the Figure 3, we see that as ε_2 decreases, both algorithms demonstrate the convergence to almost the same solution. The value ε_1 tends to zero with the same rate. This convinces us of the correctness of the **FDMSk** technique.

Here, we also note the advantages of the finite difference scheme over Monte Carlo methods (see Table 3). If the high accuracy of solution is necessary (e.g., better than 10^{-2}), the novel **FDMSk** approach achieves it significantly faster than **LRMC**.

ε_2	K_{ij}^2		K_{ij}^3	
	LRMC [sec]	FDMSk [sec]	LRMC [sec]	FDMSk [sec]
10^{-1}	0.28	0.7	0.034	9.76
10^{-2}	9.2	2.1	3.6	10.569
10^{-3}	821	7.5	315.6	23.821
10^{-4}	77 975 (≈ 21 hours)	8.2	27 192 (≈ 7.5 hours)	54.490
10^{-5}	7 908 827 (≈ 91 days)	30.08	2 599 938 (≈ 30 days)	129.692

Table 3: The running time of the algorithms under different accuracy requirements ε_2

The other important advantage of **FDMSk** is its efficiency while operating with a large number of equations. It becomes necessary if we have a wide range of particle sizes. For example, consider a system with the following initial conditions:

$$n_k(t = 0) = \begin{cases} \frac{1}{k+1}, & k \leq M, \\ 0, & k > M. \end{cases}$$

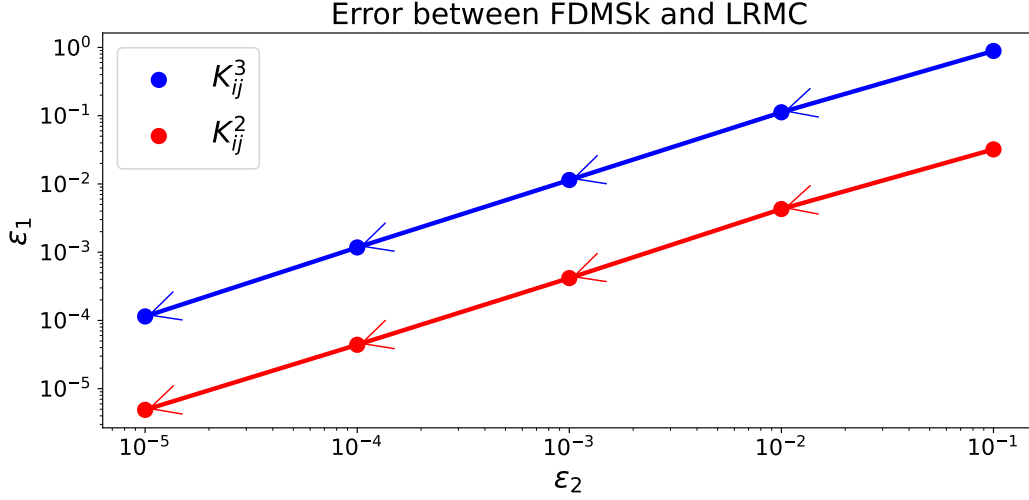


Figure 3: The mutual error ϵ_1 of the FDMSk and LRMC with increasing accuracy ϵ_2 of each of them for kernels K_{ij}^2, K_{ij}^3 . Linear decreasing of mutual error is observed.

Here, or testing on a computationally intensive case we set the maximal particle size as $M = 10^6$ and consider the target dimensionless time stamp $t = 1$.

The disadvantage of the LRMC method is its ambiguity in choosing a low-rank majorant for the kernel. For many well-known kernels, it is easy to write out a majorant that will asymptotically allow a high acceptance rate. However, for example, for the K_{ij}^3 , we hypothesize that it is impossible to construct an asymptotically correct low-rank majorant. Unfortunately, our majorant \hat{K}_{ip}^3 has a poor acceptance rate:

$$\lim_{i \rightarrow +\infty} P(\text{Accept} \mid \{i, p\}) = \lim_{i \rightarrow +\infty} \frac{K_{ip}^3}{\hat{K}_{ip}^3} = \lim_{i \rightarrow +\infty} \frac{1}{i} = 0, \quad p \in \mathbb{N}$$

This fact is confirmed numerically by the experiment. The running time of the FDMSk algorithm with adaptive time-step selection in the Runge-Kutta scheme takes **2782 seconds**. Meanwhile, one run of the LRMC with $V = 10^6$ simulation requires **53 hours** and the acceptance rate is $2 \cdot 10^{-5}$. This demonstrates the best side of the proposed FDMSk method and demonstrates its extremely good properties in solving truly large systems.

4.3 Complexity analysis

In this section we verify the theoretical estimates of the complexity of the FDMSk algorithm in practice. Recall that the estimate (13) on the algorithmic complexity for each time step of the FDMSk method is

$$\mathcal{C}_{f_1+f_2}(M) = \mathcal{O}(RM \log^2 M).$$

It consists of evaluation of the operators f_1 and f_2 with complexities $\mathcal{O}(RM \log^2 M)$ and $\mathcal{O}(RM \log M)$, respectively, see Eqs. (12) and (10).

In the experiment we study the performance of our code on the evaluation of f_1 and f_2 in the case of kernel K_{ij}^3 . On Figure 4 an excellent agreement of the theoretical estimates with the actual performance of the algorithm is demonstrated for two different mosaic partitionings. Precise running time values can be found in Table 4. Note that calculations with $M = 2^{20}$ require modest amount of time and can be performed on a personal computer.

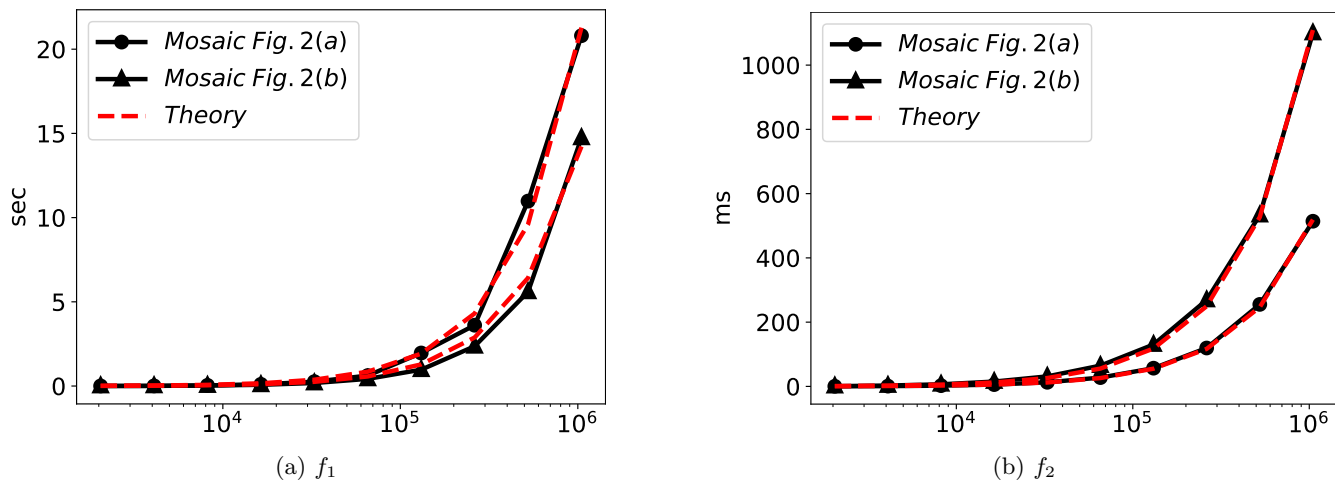


Figure 4: Evaluation time of the operators f_1 and f_2 in mosaic-skeleton format compared to the theoretical estimates.

M	f_1 [sec] Figure 2a	f_2 [ms] Figure 2a	f_1 [sec] Figure 2b	f_2 [ms] Figure 2b
2^{11}	0.0048	0.3580	0.0022	0.8576
2^{12}	0.0078	0.8352	0.0081	2.7439
2^{13}	0.0377	2.2932	0.0290	6.5832
2^{14}	0.1002	5.6186	0.0728	15.080
2^{15}	0.2591	12.820	0.1796	31.206
2^{16}	0.6207	27.435	0.4245	64.712
2^{17}	1.9605	56.718	0.9710	130.33
2^{18}	3.6114	119.53	2.3615	269.00
2^{19}	10.980	255.25	5.5937	533.12
2^{20}	20.804	514.06	14.737	1099.9

Table 4: Operation time in mosaic-skeleton format for the operators f_1, f_2 for K_{ij}^3 .

5 Conclusion and future work

In this work we demonstrate that the mosaic-skeleton matrix format allows to approximate the broad family of coagulation kernels. The novel method allows to evaluate the Smoluchowski operator numerically within $\mathcal{O}(RM \log^2 M)$ operations. It make possible to simulate aggregation process even for the wide particle size distributions and for the kernels with formally high ranks. We incept these new fast methods into the classical Runge-Kutta methods and verify their accuracy in comparison with the Monte Carlo LRMC approach. The tests of our approach are presented with using up to $M = 2^{20}$ nonlinear equations.

The developed methodology is implemented as an open-source software and allows the researchers to use our approach as a blackbox solver, setting only the coagulation kernel and initial conditions. In the future, we plan to study if the mosaic-skeleton approximations could be also useful for accelerating the Monte Carlo methods.

Acknowledgements

This work is supported by Russian Science Foundation, Project 25-21-00047 (the project webpage is available <https://rscf.ru/project/25-21-00047/>). Authors are grateful to Alexander Osinsky for useful discussions.

References

- [1] P. L. Krapivsky, S. Redner, and E. Ben-Naim, *A kinetic view of statistical physics*. Cambridge University Press, 2010.
- [2] P. J. Flory, “Molecular size distribution in three dimensional polymers. I. Gelation,” *Journal of the american chemical society*, vol. 63, no. 11, pp. 3083–3090, 1941.
- [3] V. Skorych, M. Dosta, E.-U. Hartge, S. Heinrich, R. Ahrens, and S. Le Borne, “Investigation of an fft-based solver applied to dynamic flowsheet simulation of agglomeration processes,” *Advanced powder technology*, vol. 30, no. 3, pp. 555–564, 2019.
- [4] S. Friedlander, *Smoke, Dust, and Haze: Fundamentals of Aerosol Dynamics*. Topics in chemical engineering, Oxford University Press, 2000.
- [5] S. Matveev, P. Krapivsky, A. Smirnov, E. Tyrtysnikov, and N. V. Brilliantov, “Oscillations in aggregation-shattering processes,” *Physical review letters*, vol. 119, no. 26, p. 260601, 2017.
- [6] P. Erdős, A. Rényi, *et al.*, “On the evolution of random graphs,” *Publ. math. inst. hung. acad. sci.*, vol. 5, no. 1, pp. 17–60, 1960.
- [7] S. Janson, D. E. Knuth, T. Łuczak, and B. Pittel, “The birth of the giant component,” *Random Structures & Algorithms*, vol. 4, no. 3, pp. 233–358, 1993.
- [8] A. A. Lushnikov, “Time evolution of a random graph,” *J. Phys. A*, vol. 38, no. 46, pp. L777–L782, 2005.
- [9] D. J. Aldous, “Deterministic and stochastic models for coalescence (aggregation and coagulation): A review of the mean-field theory for probabilists,” *Bernoulli*, vol. 5, no. 1, p. 3, 1999.
- [10] S. N. Dorogovtsev and J. F. Mendes, *Evolution of networks: From biological nets to the Internet and WWW*. Oxford university press, 2003.
- [11] M. v. Smoluchowski, “Versuch einer mathematischen Theorie der Koagulationskinetik kolloider Lösungen,” *Zeit. Physikalische Chemie*, vol. 92, no. 1, pp. 129–168, 1918.
- [12] M. v. Smoluchowski, “Drei vortrage uber diffusion, Brownsche bewegung und koagulation von kolloidteilchen,” *Zeit. Physik*, vol. 17, pp. 557–585, 1916.
- [13] F. Leyvraz, “Scaling theory and exactly solved models in the kinetics of irreversible aggregation,” *Phys. Reports*, vol. 383, no. 2-3, pp. 95–212, 2003.
- [14] M. Singh, V. Ranade, O. Shardt, and T. Matsoukas, “Challenges and opportunities concerning numerical solutions for population balances: a critical review,” *Journal of Physics A: Mathematical and Theoretical*, vol. 55, no. 38, p. 383002, 2022.
- [15] S. A. Matveev, A. P. Smirnov, and E. Tyrtysnikov, “A fast numerical method for the Cauchy problem for the Smoluchowski equation,” *Journal of Computational Physics*, vol. 282, pp. 23–32, 2015.
- [16] A. Osinsky, “Low-rank method for fast solution of generalized smoluchowski equations,” *Journal of Computational Physics*, vol. 422, p. 109764, 2020.
- [17] W. Hackbusch, “On the efficient evaluation of coalescence integrals in population balance models,” *Computing*, vol. 78, pp. 145–159, 2006.
- [18] M. Singh, “Accurate and efficient approximations for generalized population balances incorporating coagulation and fragmentation,” *Journal of Computational Physics*, vol. 435, p. 110215, 2021.

- [19] K. K. Sabelfeld and G. Eremeev, “A hybrid kinetic-thermodynamic Monte Carlo model for simulation of homogeneous burst nucleation,” *Monte Carlo Methods and Applications*, vol. 24, no. 3, pp. 193–202, 2018.
- [20] F. E. Kruijs, A. Maisels, and H. Fissan, “Direct simulation Monte Carlo method for particle coagulation and aggregation,” *AIChE Journal*, vol. 46, no. 9, pp. 1735–1742, 2000.
- [21] A. Eibeck and W. Wagner, “An efficient stochastic algorithm for studying coagulation dynamics and gelation phenomena,” *SIAM Journal on Scientific Computing*, vol. 22, no. 3, pp. 802–821, 2000.
- [22] R. I. Patterson, W. Wagner, and M. Kraft, “Stochastic weighted particle methods for population balance equations,” *Journal of Computational Physics*, vol. 230, no. 19, pp. 7456–7472, 2011.
- [23] M. Goodson and M. Kraft, “An efficient stochastic algorithm for simulating nano-particle dynamics,” *Journal of Computational Physics*, vol. 183, no. 1, pp. 210–232, 2002.
- [24] M. H. Lee, “On the validity of the coagulation equation and the nature of runaway growth,” *Icarus*, vol. 143, no. 1, pp. 74–86, 2000.
- [25] V. Stadnichuk, A. Bodrova, and N. Brilliantov, “Smoluchowski aggregation–fragmentation equations: Fast numerical method to find steady-state solutions,” *International Journal of Modern Physics B*, vol. 29, no. 29, p. 1550208, 2015.
- [26] N. Yadav, M. Singh, S. Singh, R. Singh, and J. Kumar, “A note on homotopy perturbation approach for non-linear coagulation equation to improve series solutions for longer times,” *Chaos, Solitons & Fractals*, vol. 173, p. 113628, 2023.
- [27] J. Koch, W. Hackbusch, and K. Sundmacher, “H-matrix methods for quadratic integral operators appearing in population balances,” *Computers & Chemical Engineering*, vol. 32, no. 8, pp. 1789–1809, 2008.
- [28] S. A. Goreinov and E. E. Tyrtshnikov, “The maximal-volume concept in approximation by low-rank matrices,” *Contemporary Mathematics*, vol. 280, pp. 47–52, 2001.
- [29] S. A. Goreinov, I. V. Oseledets, D. V. Savostyanov, E. E. Tyrtshnikov, and N. L. Zamarashkin, “How to find a good submatrix,” in *Matrix Methods: Theory, Algorithms And Applications: Dedicated to the Memory of Gene Golub*, pp. 247–256, World Scientific, 2010.
- [30] D. A. Zheltkov and E. E. Tyrtshnikov, “A parallel implementation of the matrix cross approximation method,” *Numerical Methods and Programming (Vychislitel’nye Metody i Programirovanie)*, vol. 16, pp. 369–375, 2015.
- [31] M. Bebendorf, “Approximation of boundary element matrices,” *Numerische Mathematik*, vol. 86, pp. 565–589, 2000.
- [32] A. Chaudhury, I. Oseledets, and R. Ramachandran, “A computationally efficient technique for the solution of multi-dimensional pbms of granulation via tensor decomposition,” *Computers & chemical engineering*, vol. 61, pp. 234–244, 2014.
- [33] R. A. Horn and C. R. Johnson, *Matrix analysis*. Cambridge university press, 2012.
- [34] N. Halko, P.-G. Martinsson, and J. A. Tropp, “Finding structure with randomness: Probabilistic algorithms for constructing approximate matrix decompositions,” *SIAM review*, vol. 53, no. 2, pp. 217–288, 2011.
- [35] E. Fehlberg, “Classical fourth-and lower order Runge-Kutta formulas with stepsize control and their application to heat transfer problems,” *Computing*, vol. 6, pp. 61–71, 1970.
- [36] S. A. Matveev, V. Zhilin, and A. P. Smirnov, “Adaptive time-stepping for aggregation-shattering kinetics,” *arXiv preprint arXiv:2407.16559*, 2024.

- [37] S. A. Goreinov, E. E. Tyrtyshnikov, and N. L. Zamarashkin, “A theory of pseudoskeleton approximations,” *Linear algebra and its applications*, vol. 261, no. 1-3, pp. 1–21, 1997.
- [38] B. Beckermann and A. Townsend, “On the singular values of matrices with displacement structure,” *SIAM Journal on Matrix Analysis and Applications*, vol. 38, no. 4, pp. 1227–1248, 2017.
- [39] G. Carnevale, Y. Pomeau, and W. Young, “Statistics of ballistic agglomeration,” *Physical review letters*, vol. 64, no. 24, p. 2913, 1990.
- [40] E. Trizac and P. Krapivsky, “Correlations in ballistic processes,” *Physical review letters*, vol. 91, no. 21, p. 218302, 2003.
- [41] S. Paul and S. K. Das, “Dimension dependence of clustering dynamics in models of ballistic aggregation and freely cooling granular gas,” *Physical Review E*, vol. 97, no. 3, p. 032902, 2018.
- [42] F. Lai, S. Friedlander, J. Pich, and G. Hidy, “The self-preserving particle size distribution for brownian coagulation in the free-molecule regime,” *Journal of Colloid and Interface Science*, vol. 39, no. 2, pp. 395–405, 1972.
- [43] M. Thorn and M. Seesselberg, “Dynamic scaling in colloidal aggregation: Comparison of experimental data with results of a stochastic simulation,” *Physical review letters*, vol. 72, no. 22, p. 3622, 1994.
- [44] G. Odriozola, R. Leone, A. Schmitt, J. Callejas-Fernández, R. Martinez-Garcia, and R. Hidalgo-Alvarez, “Irreversible versus reversible aggregation: Mean field theory and experiments,” *The Journal of chemical physics*, vol. 121, no. 11, pp. 5468–5481, 2004.
- [45] R. R. Dyachenko, S. A. Matveev, and P. L. Krapivsky, “Finite-size effects in addition and chipping processes,” *Physical Review E*, vol. 108, no. 4, p. 044119, 2023.
- [46] Y. Liao and D. Lucas, “A literature review on mechanisms and models for the coalescence process of fluid particles,” *Chemical Engineering Science*, vol. 65, no. 10, pp. 2851–2864, 2010.
- [47] C. Sheng and X. Shen, “Simulation of acoustic agglomeration processes of poly-disperse solid particles,” *Aerosol Science and Technology*, vol. 41, no. 1, pp. 1–13, 2007.
- [48] J. Floyd, K. Overholt, and O. Ezekoye, “Soot deposition and gravitational settling modeling and the impact of particle size and agglomeration,” *Fire Safety Science*, vol. 11, p. 174, 2014.
- [49] I. Derevich, “Coagulation kernel of particles in a turbulent gas flow,” *International Journal of Heat and Mass Transfer*, vol. 50, no. 7-8, pp. 1368–1387, 2007.
- [50] A. Osinsky and N. Brilliantov, “Hydrodynamic equations for space-inhomogeneous aggregating fluids with first-principle kinetic coefficients,” *Physical Review Letters*, vol. 133, no. 21, p. 217201, 2024.
- [51] M. Kostoglou, T. D. Karapantsios, and O. Oikonomidou, “A critical review on turbulent collision frequency/efficiency models in flotation: Unravelling the path from general coagulation to flotation,” *Advances in Colloid and Interface Science*, vol. 279, p. 102158, 2020.
- [52] V. V. Voevodin, “On a method of reducing the matrix order while solving integral equations,” in *Numerical Analysis on FORTRAN*, (Moscow University Press), pp. 21–26, 1979.
- [53] W. Hackbusch and Z. P. Nowak, “On the fast matrix multiplication in the boundary element method by panel clustering,” *Numerische Mathematik*, vol. 54, no. 4, pp. 463–491, 1989.
- [54] W. Hackbusch *et al.*, *Hierarchical matrices: algorithms and analysis*, vol. 49. Springer, 2015.
- [55] E. Tyrtyshnikov, “Mosaic-skeleton approximations,” *Calcolo*, vol. 33, pp. 47–57, 1996.

- [56] B. Valiakhmetov and E. Tyrtysnikov, “MSk - the package for a dense matrix approximation in the mosaic-skeleton format,” in *Russian Supercomputing Days : Proceedings of the International Conference*, (Moscow, Russia), pp. 20–27, September 25–26 2023.
- [57] E. Tyrtysnikov, “Incomplete cross approximation in the mosaic-skeleton method,” *Computing*, vol. 64, pp. 367–380, 2000.
- [58] P. Horvai, S. Nazarenko, and T. H. Stein, “Coalescence of particles by differential sedimentation,” *Journal of Statistical Physics*, vol. 130, pp. 1177–1195, 2008.
- [59] G. Casamatta and A. Vogelpohl, “Modelling of fluid dynamics and mass transfer in extraction columns,” *German chemical engineering*, vol. 8, no. 2, pp. 96–103, 1985.
- [60] R. Zagidullin, A. P. Smirnov, S. Matveev, N. V. Brilliantov, and P. L. Krapivsky, “Aggregation in non-uniform systems with advection and localized source,” *Journal of Physics A: Mathematical and Theoretical*, vol. 55, no. 26, p. 265001, 2022.
- [61] C. Coulaloglou and L. L. Tavlarides, “Description of interaction processes in agitated liquid-liquid dispersions,” *Chemical Engineering Science*, vol. 32, no. 11, pp. 1289–1297, 1977.
- [62] V. Khmelev, A. Shalunov, S. Tsyganok, and P. Danilov, “Smoke precipitation by exposure to dual-frequency ultrasonic oscillations,” *Fire*, vol. 7, no. 12, p. 476, 2024.
- [63] V. Khmelev, A. Shalunov, and R. Golykh, “Mathematical simulation of the influence of acoustic on the efficiency of pm 2.5 coagulation,” *Mathematics*, vol. 12, no. 5, p. 692, 2024.
- [64] M. Konno, T. MUTO, and S. Saito, “Coalescence of dispersed drops in an agitated tank,” *Journal of chemical engineering of Japan*, vol. 21, no. 4, pp. 335–338, 1988.
- [65] H. Luo, *Coalescence, breakup and liquid circulation in bubble column reactors*. PhD thesis, The Norwegian Institute of Technology, Trondheim, June 1995.
- [66] A. Osinsky, “Low-rank Monte Carlo for Smoluchowski-class equations,” *Journal of Computational Physics*, vol. 506, p. 112942, 2024.
- [67] “INM RAS cluster.” <https://cluster2.inm.ras.ru/en/>, May 2024. Date: 01.05.2024.